Binding and transition energies of shallow impurities in cylindrical GaAs quantum-well wires under a uniform magnetic field

1998 J. Phys.: Condens. Matter 10 10599

(http://iopscience.iop.org/0953-8984/10/47/011)

J. Phys.: Condens. Matter **10** (1998) 10599–10612. Printed in the UK PII: S0953-8984(98)94705-1

Binding and transition energies of shallow impurities in cylindrical GaAs quantum-well wires under a uniform magnetic field

Pablo Villamil† and N Porras-Montenegro‡

† Departamento de Matemáticas y Física, Universidad de Sucre, AA 406, Sincelejo, Colombia
‡ Departamento de Física, Universidad del Valle, AA 25360, Cali, Colombia

Received 2 June 1998, in final form 4 September 1998

Abstract. We report a calculation of the binding and transition energies of the ground and some excited states of a hydrogenic donor impurity located at the axis of a cylindrical GaAs quantum-well wire, under the action of a magnetic field applied in the axial direction. Calculations are made using the effective-mass approximation within the variational approach for infinite confinement potential. Our results are obtained for several wire radii and as a function of the applied magnetic field. We have found that some excited states are not bounded for some values of the radius of the wire and of the applied magnetic field. We show how the geometric confinement and the applied magnetic field split the degeneracy of some excited states. Also, we compare our results with those found in GaAs–(Ga, Al)As quantum wells.

1. Introduction

The great progress in semiconductor nanotechnology, such as molecular beam epitaxy (MBE), metal–organic chemical-vapour deposition (MOCVD) and chemical lithography, has made possible the realization of a wide variety of semiconductor heterostructures, where the quantum mechanical nature of the electrons plays an important role. The effects of applied magnetic fields on the physical properties of low dimensional systems are studied with interest from the theoretical and experimental point of view. These studies have been performed with the proposal of understanding the fascinating novel phenomena and of creating new devices with other functions or to improve the performance of the existing ones. Although magnetic field effects seem to have less technological significance, they provide a far richer insight into semiconductor physics than is possible by studying electrons in electric fields. Magnetic fields have become crucial ingredients of characterization techniques used to evaluate semiconductor physics.

The magnetic field greatly alters the nature of the electronic states, which manifest themselves in magneto-optic or magneto-transport phenomenon. Magneto-spectroscopy experiments have been carried out on shallow donor impurities doped in the central region of a GaAs quantum wells (QWs) in a GaAs–$Ga_{1-x}Al_xAs$ multiple QWs by Jarosik *et al* [1], who found increased values for the $1s–2p_{\pm}$ transition energies with respect to the bulk values. Far infrared measurements performed by Yoo *et al* [2] have allowed the observation of electric-field effects on the electronic states of shallow impurities in selectively donor doped $Ga_{1-x}Al_xAs$ QWs. The effects of electric and magnetic fields on the intradonor transition energies between the 1s-like ground state and $2p_{\pm}$-like excited states of a hydrogenic donor

0953-8984/98/4710599+14$19.50

impurities were recently studied by Latgé *et al* [3] following a variational calculation within the effective-mass approximation. The theoretical infrared-absorption spectra associated with $1s–2p_{\pm}$ donor transitions in GaAs–$Ga_{1-x}Al_xAs$ QWs under electric and magnetic fields, and for x-polarized radiation, were calculated taking into account the appropriate doping profile and have provided an adequate understanding of the available $1s–2p_{\pm}$ experimental measurements.

Branis *et al* [4] reported, for the first time, a calculation of the binding energy of the ground state of a hydrogenic donor impurity in a quantum wire in the presence of a uniform magnetic field applied parallel to the wire axis. The calculations were performed using suitable variational wave functions for an infinite confinement potential. They found that, for a given value of the magnetic field, the binding energy is found to be larger than in the zero-field case. Many authors have worked on the calculation of the binding energies, density of impurity states, transition energies and photoluminescence spectra associated with shallow impurities in GaAs–$Ga_{1-x}Al_xAs$ QWWs. However, there are no theoretical studies considering the effects of applied magnetic fields on the infrared transitions between excited states of donor impurities in cylindrical GaAs QWWs.

In this work, using the effective-mass approximation within the variational approach, we calculate the binding energy and some transition energies associated with the ground and some excited states of a hydrogenic donor impurity located at the axis of a cylindrical GaAs QWW, under the action of a magnetic field applied in the axial direction. The quantum wire length is enough to consider that the carrier motion is free in the axial direction. In section 2 we present the theory followed for this calculation. Our results and discussion are presented in section 3, and conclusions in section 4.

2. Theory

In the effective-mass approximation the Hamiltonian of a donor impurity located at the axis of a cylindrical GaAs QWW with radius R, infinite confinement potential and in the presence of an applied magnetic field can be written as:

$$H = \frac{1}{2m^*}\left[P - \frac{e}{c}A\right]^2 - \frac{e^2}{\varepsilon r} + V(\rho) \tag{1}$$

where $r = (\rho^2 + z^2)^{1/2}$, z is the relative coordinate of the separation between the electron and the ion of the impurity in the axial direction of the wire, ε is the dielectric constant of the GaAs, m^* is the electron effective mass, $\boldsymbol{A}(\boldsymbol{r})$ is the potential vector of the magnetic field and $V(\rho)$ is the confinement potential defined as

$$V(\rho) = \begin{cases} 0 & 0 \leqslant \rho \leqslant R \\ \infty & \rho > R \end{cases} \tag{2}$$

$V(z) = 0$ for all z.

The vector potential is written as $\boldsymbol{A}(\boldsymbol{r}) = \frac{1}{2}(\boldsymbol{B} \times \boldsymbol{r})$, with $\boldsymbol{B} = B\boldsymbol{z}$. In cylindrical coordinates the components of the vector potential are

$$A_\rho = A_z = 0 \qquad A_\varphi = \tfrac{1}{2}(B\rho). \tag{3}$$

The Hamiltonian of the system can be written in cylindrical coordinates and in effective Rydbergs as

$$H = \nabla^2 - \mathrm{i}\gamma\left(\frac{\partial}{\partial\varphi}\right) + \frac{\gamma^2\rho^2}{4} - \frac{2}{r} + V(\rho) \tag{4}$$

where we have used the atomic units of length $a^* = \hbar^2\varepsilon/m^*e^2$ and energy $R^* = e^2/2\varepsilon a^*$. In equation (4), γ is the measure of the electron energy in the first Landau level ($n = 0$), due to the action of the magnetic field, which is expressed by $\gamma = e\hbar B/2m^*cR^*$. For donor impurities in GaAs, $m^* = 0.065$, $\varepsilon = 12.58$, $a^* \cong 100$ Å and $R^* = 5.83$ meV.

Due to the inclusion of the impurity potential in the Hamiltonian, equation (1), the Schrödinger equation cannot be analytically solved. We use the variational method in order to calculate the eigenvalues of the Hamiltonian. Following Brown and Spector [5], we assume suitable variational wave functions, for the different states, as the product of a hydrogenic part with the appropriate confluent hypergeometric function. The latter part is the radial solution of an electron in an infinite potential cylindrical wire, in the presence of a magnetic field, that is

$$\psi_{nlm}(r) = \begin{cases} N_{nlm}\,{}_1F_1(a_{01}, 1; \xi)\Gamma_{nlm}(r, \{\lambda_{nl}, \beta_{nl}, \alpha_{nl}\}) & \rho \leqslant R \\ 0 & \rho > R. \end{cases} \tag{5}$$

In equation (5), N_{nlm} is the normalization constant, ${}_1F_1(a_{01}, 1, \xi)$ is the confluent hypergeometric function, with $\xi = eB\rho^2/(2\hbar c)$, a_{01} is the eigenvalue of the ground state without the impurity, which is calculated numerically from the boundary-condition for $\rho = R$,

$${}_1F_1(a_{01}, 1, \xi_R) = 0 \tag{6}$$

where $\xi_R = \gamma R^2/2a^{*2}$ and Γ_{nlm} is the hydrogenic wave function, corresponding to the nlm state, as was proposed by Latgé *et al* [6]. The λ_{nl}, β_{nl} and α_{nl} are variational parameters used by Chaudhuri and Bajaj [7] that vary according to λ_{nl} in such a way that the orthogonalization is preserved.

Following Greene and Bajaj [8] we calculate the binding energy of a given state Ψ_{nlm} by means of

$$E_{b,nlm} = \gamma(1 - 2a_{01}) - \langle H(R, B)\rangle. \tag{7}$$

The binding energy, $E_{b,nlm}$, is a positive quantity, which is measured with respect to the first energy level of the system without the impurity. The expected value of the Hamiltonian is the sum of the expected values of the kinetic $\langle T\rangle$, potential $\langle V\rangle$, diamagnetic $\langle D\rangle$, and paramagnetic $\langle P\rangle$ energies.

$$\langle H(R, B)\rangle = \langle T\rangle + \langle V\rangle + \langle D\rangle + \langle P\rangle. \tag{8}$$

Numerical calculations have been performed by setting $\rho = Rt$. The normalization constant of the 2s-like state is given by

$$N^2 = \frac{1}{[2\pi(A + B + C)]} \tag{9}$$

where A, B and C are written as

$$\begin{aligned} A &= \frac{1}{\lambda_{2s}^2}[\beta^2 - 2\beta\lambda_{2s} + 2\lambda_{2s}^2]R^3 \int_0^1 t^2\,{}_1F_1^2(a_{01}, 1; \xi_R t^2)K_1(2\lambda_{2s}Rt)\,\mathrm{d}t \\ B &= \frac{\beta}{\lambda_{2s}^2}[\beta - 4\beta\lambda_{2s}]R^4 \int_0^1 t^3\,{}_1F_1^2(a_{01}, 1; \xi_R t^2)K_0(2\lambda_{2s}Rt)\,\mathrm{d}t \\ C &= 2\beta^2R^5 \int_0^1 t^4\,{}_1F_1^2(a_{01}, 1; \xi_R t^2)K_1(2\lambda_{2s}Rt)\,\mathrm{d}t \\ \beta &= \frac{\lambda_{2s} + \lambda_{1s}}{3}. \end{aligned} \tag{10}$$

The expressions of $\langle V\rangle$, $\langle D\rangle$ and $\langle T\rangle$ are given by

$$\begin{aligned}\langle V\rangle = -4\pi N^2 a^*\Bigg[&2\beta^2 R^4\int_0^1 t^3\,{}_1F_1^2(a_{01},1;\xi_R t^2)K_0(2\lambda_{2s}Rt)\,\mathrm{d}t+\left(\frac{\beta}{\lambda_{2s}}\right)(\beta-4\lambda_{2s})R^3\\&\times\int_0^1 t^2\,{}_1F_1^2(a_{01},1;\xi_R t^2)K_1(2\lambda_{2s}Rt)\\&+2R^2\int_0^1 t\,{}_1F_1^2(a_{01},1;\xi_R t^2)K_0(2\lambda_{2s}Rt)\,\mathrm{d}t\Bigg]\end{aligned}\tag{11}$$

$$\begin{aligned}\langle D\rangle = \frac{\pi N^2\gamma^2}{2a^{*2}}\Bigg[&\left(\frac{1}{\lambda_{2s}^2}\right)(\beta^2-2\beta\lambda_{2s}+2\lambda_{2s}^2)R^5\int_0^1 t^4\,{}_1F_1^2(a_{01},1;\xi_R t^2)K_1(2\lambda_{2s}Rt)\,\mathrm{d}t\\&+\left(\frac{\beta}{\lambda_{2s}}\right)(\beta-4\lambda_{2s})R^6\int_0^1 t^5\,{}_1F_1^2(a_{01},1;\xi_R t^2)K_0(2\lambda_{2s}Rt)\,\mathrm{d}t\\&+2\beta^2R^7\int_0^1 t^6\,{}_1F_1^2(a_{01},1;\xi_R t^2)K_1(2\lambda_{2s}Rt)\,\mathrm{d}t\Bigg]\end{aligned}\tag{12}$$

$$\begin{aligned}\langle T\rangle = -2\pi N^2 a^{*2}\Bigg[&-4(\lambda_{2s}+\beta)R^2\int_0^1 t\,{}_1F_1^2(a_{01},1;\xi_R t^2)K_0(2\lambda_{2s}Rt)\,\mathrm{d}t\\&+(\beta^2+10\lambda_{2s}\beta+2\lambda_{2s}^2)R^3\int_0^1 t^2\,{}_1F_1^2(a_{01},1;\xi_R t^2)K_1(2\lambda_{2s}Rt)\,\mathrm{d}t\\&-\lambda_{2s}\beta(7\beta+4\lambda_{2s})R^4\int_0^1 t^3\,{}_1F_1^2(a_{01},1;\xi_R t^2)K_0(2\lambda_{2s}Rt)\,\mathrm{d}t\\&+2\beta^2\lambda_{2s}R^5\int_0^1 t^4\,{}_1F_1^2(a_{01},1;\xi_R t^2)K_1(2\lambda_{2s}Rt)\,\mathrm{d}t+\left(\frac{4a_{01}\vartheta}{\lambda_{2s}^2}\right)\\&\times(\beta^2-2\beta\lambda_{2s}+2\lambda_{2s}^2)R^3\int_0^1 t^2\,{}_1F_1(a_{01},1;\xi_R t^2)\,{}_1F_1(a_{01}+1,2;\xi_R t^2)\\&\times K_1(2\lambda_{2s}Rt)\,\mathrm{d}t+\left(\frac{4a_{01}\vartheta}{\lambda_{2s}}\right)(\beta^2-6\beta\lambda_{2s}-2\lambda_{2s}^2)R^4\int_0^1 t^3\,{}_1F_1(a_{01},1;\xi_R t^2)\\&\times{}_1F_1(a_{01}+1,2;\xi_R t^2)K_0(2\lambda_{2s}Rt)\,\mathrm{d}t+4a_{01}\vartheta\beta(3\beta+4\lambda_{2s})R^5\\&\times\int_0^1 t^4\,{}_1F_1(a_{01},1;\xi_R t^2)\,{}_1F_1(a_{01}+1,2;\xi_R t^2)K_1(2\lambda_{2s}Rt)\,\mathrm{d}t\\&-8a_{01}\vartheta\lambda_{2s}\beta^2R^6\int_0^1 t^5\,{}_1F_1(a_{01}+1;\xi_R t^2)\,{}_1F_1(a_{01}+1,2;\xi_R t^2)\\&\times K_0(2\lambda_{2s}Rt)\,\mathrm{d}t+\left(\frac{2a_{01}\vartheta^2}{\lambda_{2s}^2}\right)(1+a_{01})(\beta^2-2\beta\lambda_{2s}+2\lambda_{2s}^2)R^5\\&\times\int_0^1 t^4\,{}_1F_1(a_{01},1;\xi_R t^2)\,{}_1F_1(a_{01}+2,3;\xi_R t^2)K_1(2\lambda_{2s}Rt)\,\mathrm{d}t\\&+\left(\frac{2a_{01}\beta\vartheta^2}{\lambda_{2s}}\right)(1+a_{01})(\beta-4\beta\lambda_{2s})R^6\int_0^1 t^5\,{}_1F_1(a_{01},1;\xi_R t^2)\\&\times{}_1F_1(a_{01}+2,3;\xi_R t^2)K_0(2\lambda_{2s}Rt)\,\mathrm{d}t+(4a_{01}\vartheta^2\beta^2)(1+a_{01})R^7\\&\times\int_0^1 t^6\,{}_1F_1(a_{01},1;\xi_R t^2)\,{}_1F_1(a_{01}+2,3;\xi_R t^2)K_1(2\lambda_{2s}Rt)\,\mathrm{d}t\Bigg]\end{aligned}\tag{13}$$

where

$$\vartheta=\frac{\gamma}{2a^{*2}}.$$

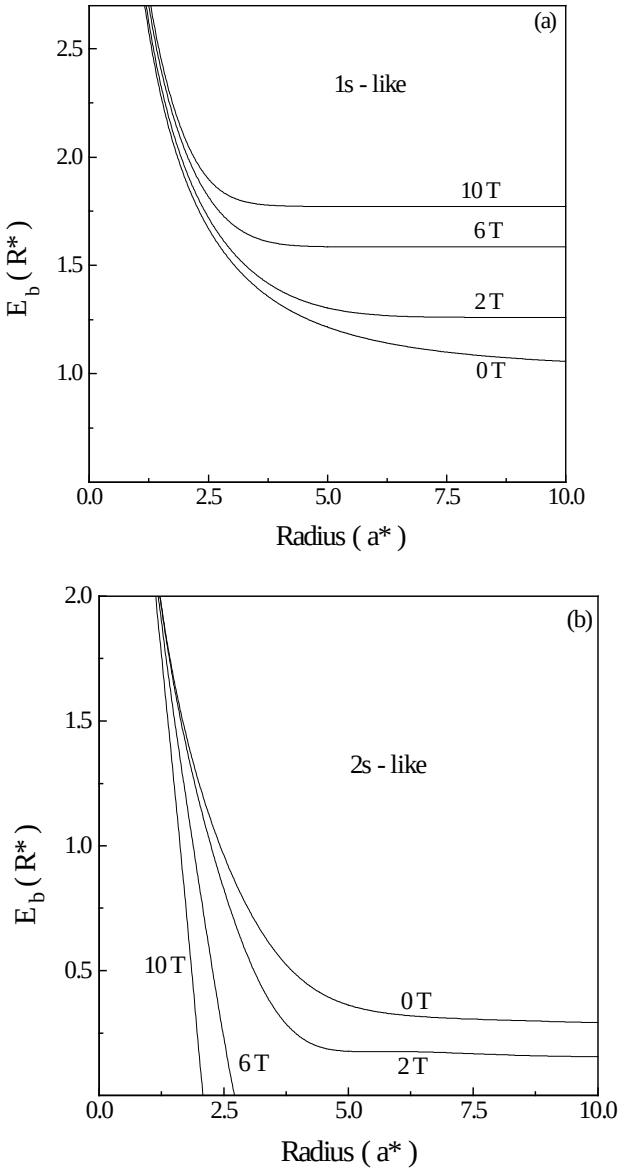

Figure 1. Binding energy of the 1s-like, 2s-like, 3s-like states of a donor impurity located at the centre of a cylindrical GaAs QWW, as a function of the wire radius, and for different values of the magnetic field.

The allowed transition energies are given by

$$E_T(nlm \to n'l'm') = |E_{b,nlm}(R, B) - E_{b,n'l'm'}(R, B)| \tag{14}$$

and the selection rules used for the allowed transitions are [3]:

$$\begin{aligned} &\Delta l = l - l' = \pm 1 \\ &\Delta m = m - m' = 0, \pm 1. \end{aligned} \tag{15}$$

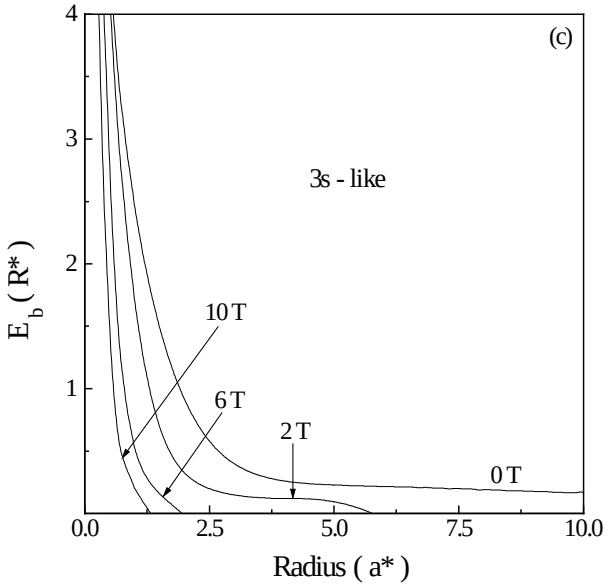

Figure 1. (Continued)

3. Results and discussion

In figure 1 we present the binding energy of the 1s-like, 2s-like and 3s-like states as a function of the radius of the wire and for different values of the applied magnetic field. For the 1s-like state we reproduce the results obtained by Branis *et al* [4]. For small values of the wire radius, $R < a^*$, the binding energy of the three states increases significantly and it is relatively insensitive to the magnetic field, because the diamagnetic energy tends to zero and the kinetic energy of the electron increases drastically, surpassing the attractive potential of the impurity. In this range of radius and for any value of the magnetic field the geometric confinement prevails over the magnetic one.

For $R \sim a^*$ the effect of the magnetic field begins to be apparent, increasing the binding energy, which tends to the bulk value for $R \sim 10a^*$. For the 1s-like state and for $B = 0$ T, our results agree with those of Aldrich and Greene [9], Brown and Spector [5] and Latgé *et al* [6]. For large values of the radius, $R > a^*$, the magnetic field determines the behaviour of the binding energy for all the ns-like states. The expected value $\langle r \rangle$ of the 3s-like state is $\sim 13a^*$, for $B = 0$ T, so that the electron is already geometrically confined in the wire of radius $R = 10a^*$ and its binding energy is a little larger than in the bulk.

For $R \geqslant a^*$, the binding energy of the 1s-like state increases with the magnetic field, meanwhile for the 2s- and 3s-like states it decreases as shown in figures 1(a), 1(b) and 1(c). The 2s-like state is unbounded for radius smaller than $3a^*$ and for magnetic fields between $B = 6$ T and 10 T. The 3s-like state is unbounded for all magnetic fields used here. The wire radius for which it begins to be unbounded is smaller when the magnetic field is increased. The binding energies of the 2s- and 3s-like states diminish with the magnetic field, because the kinetic energy, which is comparable with the diamagnetic one, exceeds significantly the attractive potential.

The binding energies of $2p_-$- and $3p_-$-like states are presented in figure 2 as a function of the radius of the wire and for different values of the applied magnetic field. In figure 2(a) it is observed that the binding energy increases with the magnetic field. Also, it is seen

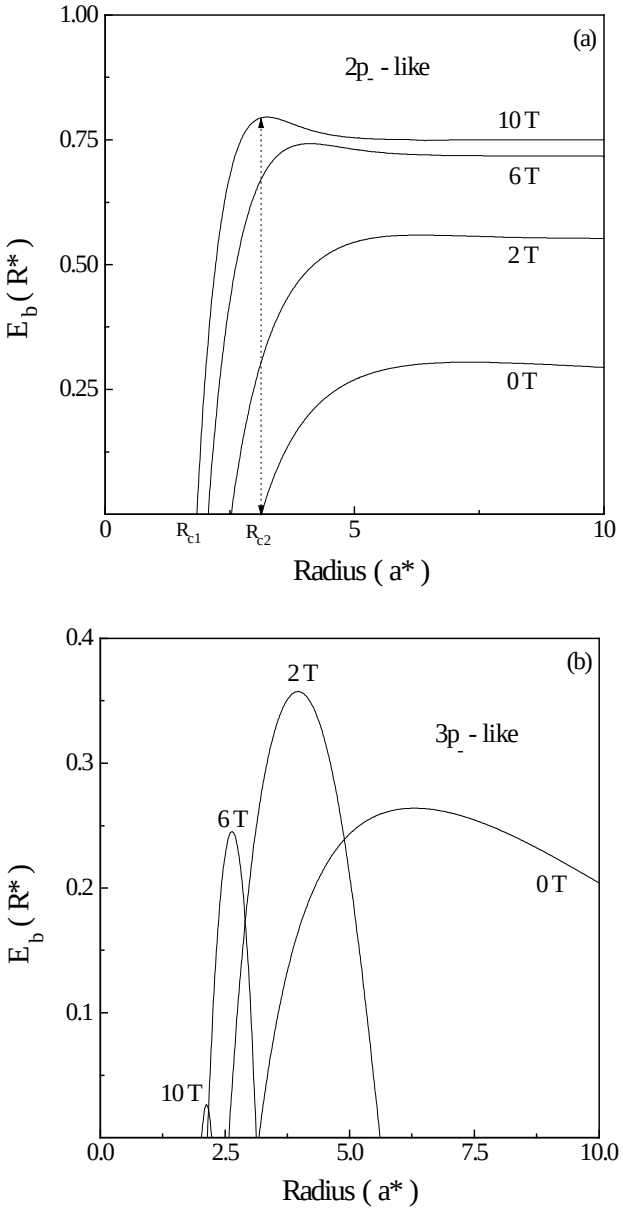

Figure 2. Binding energy of the $2p_-$-like and $3p_-$-like states of a donor impurity located at the centre of a cylindrical GaAs QWW, as a function of the wire radius, and for different values of the magnetic field.

that there are two characteristic radii $R_{c1}(B)$ (beyond this radius the states are bounded) and $R_{c2}(B)$ (for which the binding energy reaches its maximum value). Both characteristic radii diminish with increasing B and their values lie in the range of strong and intermediate geometrical confinement. For QWW radii $R_{c1}(B) < R < R_{c2}(B)$, the binding energy increases with R and the slope of the curve becomes larger when the magnetic field is augmented. The existence of the critical radius R_{c1} is due to the strong confinement of the

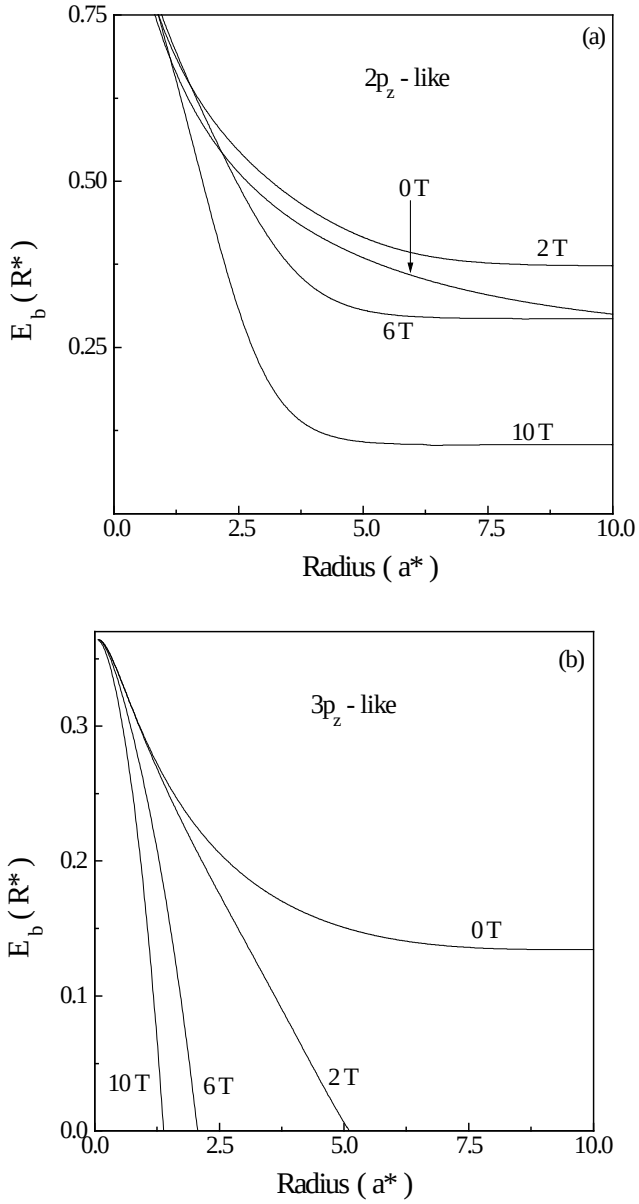

Figure 3. Binding energy of the $2p_z$-like and $3p_z$-like states of a donor impurity located at the centre of a cylindrical GaAs QWW, as a function of the wire radius, and for different values of the magnetic field.

wave function in the radial direction and therefore the corresponding energy is higher than the first ionization level within the structure (the first Landau level).

In figure 2(b) we see that the $3p_-$-like state is very sensitive to the magnetic field for large and small radius. Any increment in the value of the magnetic field makes the state bounded for smaller radius. It is observed that the radius range in which the $3p_-$-like state is bounded decreases and begins at a smaller radius with increasing magnetic field.

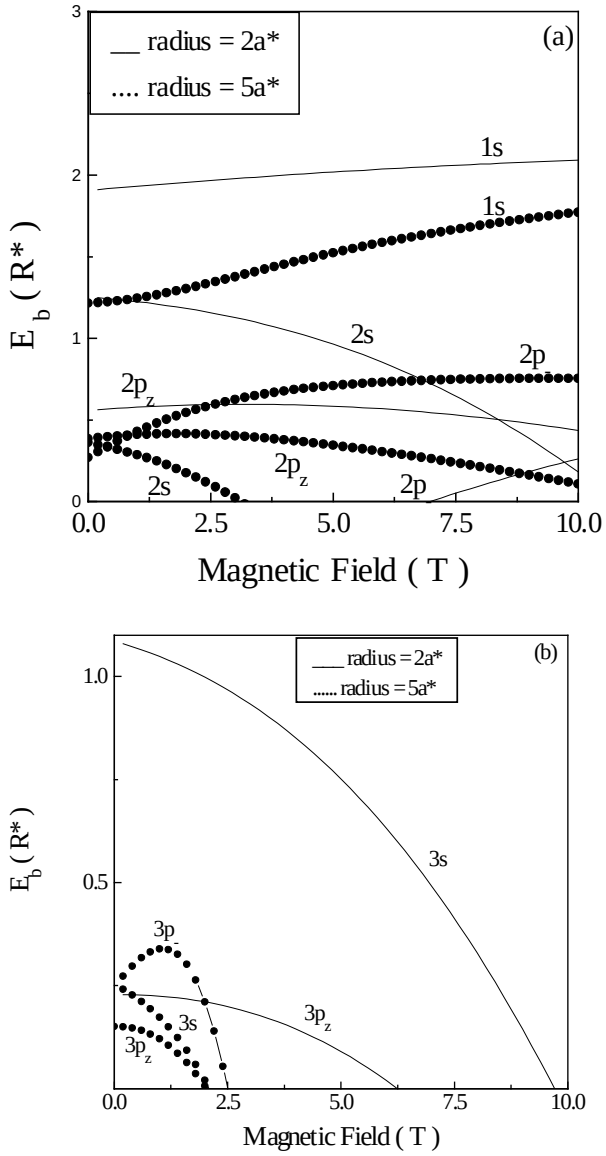

Figure 4. Binding energy of some excited states of a donor impurity located at the centre of a cylindrical GaAs QWW, as a function of the magnetic field for $R = 2a^*$, and $R = 5a^*$.

In figure 3 we plot the binding energy for the $2p_z$-like and $3p_z$-like states, versus the radius of the wire and for different values of the magnetic field. We observe that for small radius of the wire the binding energy tends to a maximum value of $1R^*$ for the $2p_z$-like state and $0.37R^*$ for the $3p_z$-like state. When the radius of the wire is large in figure 3(a) it is seen that the binding energy reaches its maximum value for $B = 2$ T. For higher values of B the binding energy diminishes. In the weak and medium geometrical confinement the binding energy is approximately constant due to the fact that $\langle T \rangle$ and $\langle V \rangle$ are also constants

for these ranges of the radius. In figure 3(b) we present the $3p_z$-like state. This state is unbounded for smaller radius as the magnetic field is increased. In this case $\langle T \rangle$ exceeds the attractive potential energy.

In figures 4(a) and 4(b) we plot the binding energy versus the magnetic field, for the 1s-, 2s-, $2p_-$-, $2p_z$-, 3s-, $3p_-$-, $3p_z$-like states, in quantum well wires of radii $2a^*$ and $5a^*$, respectively. Our results agree with those of Branis *et al* [4] for the 1s-like state. For all considered states, except the $2p_-$- and $3p_-$-like states, the binding energies corresponding to the wire of radius $2a^*$ are higher than those corresponding to the wire of radius $5a^*$. For $B = 0$ T the geometrical confinement splits the degeneracy of the states with $n = 2$ and 3. This splitting is higher in the wire with smaller radius. The $3p_-$-like state is not bounded in the wire of radius $2a^*$ in the whole range of the magnetic field. Due to the wire cylindrical symmetry and the on-centre impurity location, L_z, the z component of the angular momentum operator, is conserved. Otherwise, since the Hamiltonian, equation (4), does not mix terms in ρ with z, then the crossing between the s, p_--, p_z states is allowed. In figure 4(a) we display that for the wire of radius $2a^*$ the binding energy of the 1s-like state is very insensitive to the magnetic field and is practically constant. In this case the geometrical confinement governs over the magnetic confinement. The binding energy of the 2s-like state diminishes when the magnetic field increases while the $2p_z$-like state stays nearly constant. The $2p_-$-like state is only bounded for $B \geqslant 7$ T, due to the fact that the magnetic field links the electron to the impurity despite the large values of $\langle T \rangle$ and $\langle V \rangle$ for the strong geometrical confinement when $R = 2a^*$. The 2s-like state presents a crossing with the $2p_z$-like state for $B \cong 8.5$ T and with the $2p_-$-like state for $B \cong 9.7$ T. The binding energy of the 1s-like state, for the wire of radius $5a^*$, increases with the magnetic field. It is interesting to observe that for $B = 0$ T the geometrical confinement splits the degeneracy between the 2s-like, $2p_-$-like and the $2p_z$-like states. As it is observed that the splitting between the excited states increases with the magnetic field.

In figure 4(b) it is observed that the 3s- and 3p-like states are degenerate when the radius of the wire is $5a^*$ for $B = 0$ T. There is a splitting between the $3p_z$-like state and the 3s-like and $3p_-$-like states due to the geometrical confinement. It is important to observe that for all states displayed here, the binding energy diminishes with increasing magnetic field, becoming unbounded for higher radius of the QWW.

In figure 5(a) we present the transition energies $1s \rightarrow 2p_-$ as a function of the radius of the wire for different magnetic fields. We find that for small values of the radius these transition energies are insensitive to the magnetic field and increase significantly due to the strong geometrical confinement. When $R > 5a^*$ the transition energies are independent of the radius of the wire and present some dependence on the magnetic field. In figure 5(b) the transition energies $1s \rightarrow 2p_z$ are insensitive to the magnetic field and increase significantly for $R \geqslant a^*$. For $R > 3.5a^*$ the transition energies only depend on the magnetic field.

In figure 6(a) we display the transition energies between the 1s-like state and the states with $n = 2$ and 3 as a function of the magnetic field for wires of radius $2a^*$ and $5a^*$. For $R = 2a^*$ and $B = 0$ T the transition energies $1s \rightarrow 2p_-$ and $1s \rightarrow 3p_-$ are degenerate. It is observed that this degeneracy is split by the magnetic field. All the transition energies for $B = 0$ T and $R = 2a^*$ are higher than the corresponding ones in the wire with $R = 5a^*$. The transition energies $1s \rightarrow 2p_z$ and $1s \rightarrow 3p_z$ are increased and split themselves with the magnetic field. For $R = 2a^*$ there is a crossing between the transitions $1s \rightarrow 2p_-$ and $1s \rightarrow 3p_z$ for $B \sim 7$ T and also between $1s \rightarrow 3p_-$ and $1s \rightarrow 3p_z$ for $B \sim 7.5$ T. For the wire of radius $5a^*$, when the magnetic field increases the splitting between all the transitions is augmented. There is a crossing between the transitions $1s \rightarrow 3p_-$ and $1s \rightarrow 3p_z$ for $B \sim 2.8$ T. The transition energies $1s \rightarrow 2p_-$ and $1s \rightarrow 3p_-$ diminish with the increase of

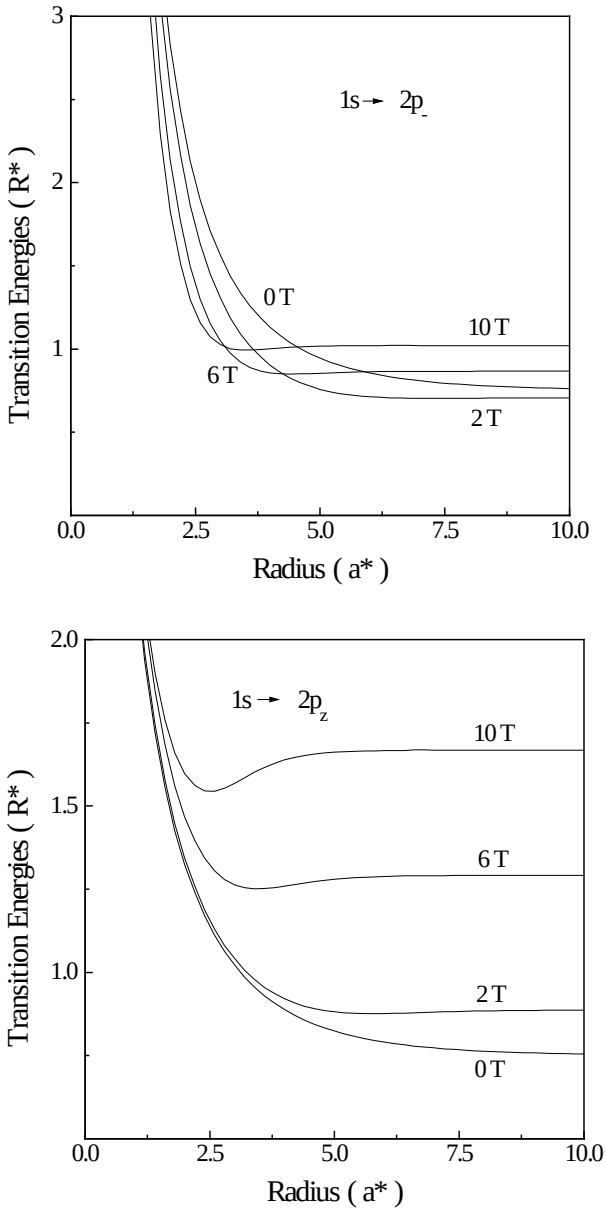

Figure 5. $1s \rightarrow 2p_{-}$ and $1s \rightarrow 2p_z$ transition energies of a donor impurity located at the centre of a cylindrical GaAs QWW, as a function of the wire radius, and for different values of the magnetic field.

the magnetic field in the wire with $R = 2a^*$, while the same transition energies present an opposite behaviour with the magnetic field in the wire with $R = 5a^*$.

In figure 6(b) we show the transition energies $2s \rightarrow 3p_{-}$ and $2s \rightarrow 3p_z$ as a function of the magnetic field for wires of radius $2a^*$ and $5a^*$, respectively. For the wire with $R = 2a^*$ both transition energies diminish with the magnetic field. There is a crossing between these two transition energies for $B \sim 7.5$ T. For the wire with $R = 5a^*$ and $B < 7.5$ T

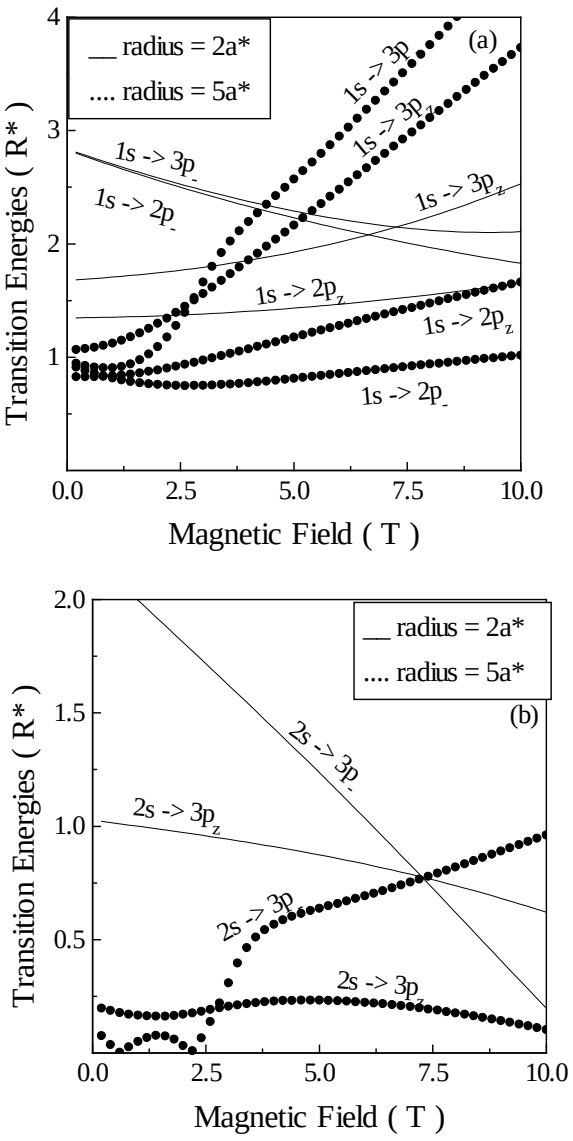

Figure 6. Infrared transition energies between some excited states of a donor impurity located at the centre of a cylindrical GaAs QWW, as a function of the magnetic field, and for different values of the wire radius.

the transition energies are smaller than those presented for the wire with $R = 2a^*$. The transition energy $2s \rightarrow 3p_-$ is reversed for magnetic fields between 1 and 2.3 T and there is a crossing between these transition energies for $B \sim 2.8$ T.

In figure 6(c) we display the transition energies $2p_- \rightarrow 3s$ and $2p_z \rightarrow 3s$ as a function of the magnetic field for wires with radius $R = 2a^*$ and $R = 5a^*$, respectively. For the wire of radius $2a^*$ the transition energy $2p_z \rightarrow 3s$ is reversed for $B \geqslant 6.5$ T, while the transition $2p_- \rightarrow 3s$ is reversed for $B \geqslant 8.5$ T. It is noticeable that for the wire of radius $5a^*$ the transition energies $2p_- \rightarrow 3s$ and $2p_z \rightarrow 3s$ increase and split with the magnetic field, in contrast to the behaviour of the transition energies in the wire with $R = 2a^*$.

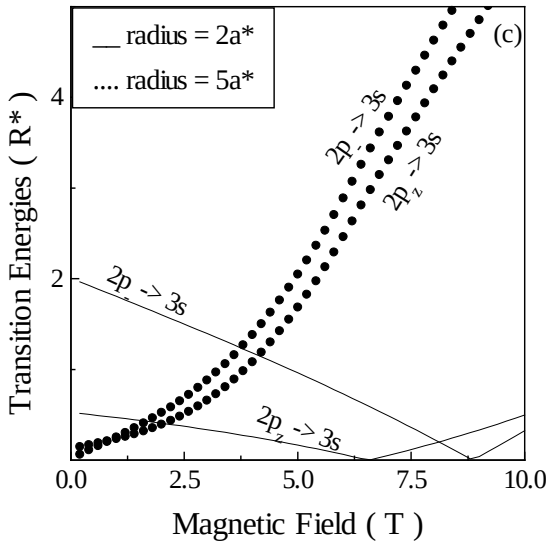

Figure 6. (Continued)

4. Conclusions

In this work and for the first time, we have considered the effects of an applied magnetic field in the binding energy of some excited states as well as the allowed transition energies between the 1s-like, 2s-like, 3s-like, $2p_-$-like, $3p_-$-like, $2p_z$-like and $3p_z$-like states of an on-centre shallow donor impurity in a cylindrical GaAs QWW. We have used the effective-mass approximation within a variational scheme and considered a magnetic field applied parallel to the axis of the wire. We have found that some excited states are not bounded for some values of the radius of the wire and of the applied magnetic field. Also, we have shown how the geometric confinement and the applied magnetic field raise the degeneracy of some excited states. Unfortunately, it is not possible to compare our results with experimental data, as measurements of the infrared transitions under applied magnetic fields have not been carried out so far in QWWs. As has been referenced, however, some theoretical and experimental work on the impurity infrared transition energies in GaAs–(Ga, Al)As quantum wells has already been done under applied magnetic fields. Considering the potential device applications of the role of impurities in semiconducting heterostructures, we believe the present calculation will be of importance in the quantitative understanding of future experimental work in this subject. Despite the fact that this work has been done for GaAs using the infinite potential model, its results could be used to discuss experimental results not only in vacuum–GaAs–vacuum, but in GaAs–$Ga_{1-x}Al_xAs$ QWWs under the action of applied magnetic fields, whenever $0.30 < x < 0.45$ in order to have high enough potential barriers.

Acknowledgment

This work was partially financed by the Colombian scientific agency, Colciencias, under the grant No 1106-05-025-96.

References

[1] Jarosik N C, McCombe B D, Shanabrook B V, Comas J, Ralston J and Wicks G 1985 *Phys. Rev. Lett.* **54** 1283
[2] Yoo B S, He L, McCombe B D and Schaff W 1991 *Superlatt. Microstruct.* **8** 297
Yoo B S, McCombe B D and Schaff W 1991 *Phys. Rev.* B **44** 13 152
[3] Latgé A, Porras-Montenegro N and Oliveira L 1995 *Phys. Rev.* B **51** 2259
[4] Branis S, Gang Li and Bajaj K 1993 *Phys. Rev.* B **47** 1316
[5] Brown J and Spector H 1986 *J. Appl. Phys.* **59** 1179
[6] Latgé A, Porras-Montenegro N and Oliveira L 1992 *Phys. Rev.* B **45** 9420
[7] Chaudhury S and Bajaj K 1984 *Phys. Rev.* B **29** 1803
[8] Greene R and Bajaj K 1988 *Phys. Rev.* B **37** 4604
[9] Aldrich C and Greene R 1979 *Phys. Status Solidi* b **93** 343
[10] Latgé A, Porras-Montenegro N, de Dios-Leyva M and Oliveira L 1996 *Phys. Rev.* B **53** 10 160
[11] Szwacka T 1996 *J. Phys.: Condens. Matter* **8** 10 521
[12] Xiao Z, Zhu J and He F 1995 *Phys. Status Solidi* b **191** 401